

In Vitro Analysis of Hrd1p-mediated Retrotranslocation of Its Multispanning Membrane Substrate 3-Hydroxy-3-methylglutaryl (HMG)-CoA Reductase^{*[S]}

Received for publication, December 22, 2008, and in revised form, March 20, 2009. Published, JBC Papers in Press, March 26, 2009, DOI 10.1074/jbc.M809607200

Renee M. Garza, Brian K. Sato, and Randolph Y. Hampton¹

From the Section of Cell and Developmental Biology, Division of Biological Sciences, University of California, San Diego, La Jolla, California 92093-0347

Endoplasmic reticulum (ER)-associated degradation (ERAD) is responsible for the ubiquitin-mediated destruction of both misfolded and normal ER-resident proteins. ERAD substrates must be moved from the ER to the cytoplasm for ubiquitination and proteasomal destruction by a process called retrotranslocation. Many aspects of retrotranslocation are poorly understood, including its generality, the cellular components required, the energetics, and the mechanism of transfer through the ER membrane. To address these questions, we have developed an *in vitro* assay, using the 8-transmembrane span ER-resident Hmg2p isozyme of HMG-CoA reductase fused to GFP, which undergoes regulated ERAD mediated by the Hrd1p ubiquitin ligase. We have now directly demonstrated *in vitro* retrotranslocation of full-length, ubiquitinated Hmg2p-GFP to the aqueous phase. Hrd1p was rate-limiting for Hmg2p-GFP retrotranslocation, which required ATP, the AAA-ATPase Cdc48p, and its receptor Ubx2p. In addition, the adaptors Dsk2p and Rad23p, normally implicated in later parts of the pathway, were required. Hmg2p-GFP retrotranslocation did not depend on any of the proposed ER channel candidates. To examine the role of the Hrd1p transmembrane domain as a retrotranslocator, we devised a self-ubiquitinating polytopic substrate (Hmg1-Hrd1p) that undergoes ERAD in the absence of Hrd1p. *In vitro* retrotranslocation of full-length Hmg1-Hrd1p occurred in the absence of the Hrd1p transmembrane domain, indicating that it did not serve a required channel function. These studies directly demonstrate polytopic membrane protein retrotranslocation during ERAD and delineate avenues for mechanistic understanding of this general process.

The endoplasmic reticulum (ER)²-associated degradation (ERAD) pathway mediates the destruction of numerous inte-

gral membrane or luminal ER-localized proteins (1, 2). ERAD functions mainly in the disposal of misfolded or unassembled proteins but also participates in the physiological regulation of some normal residents of the organelle. This ER-localized degradation pathway has been implicated in a wide variety of normal and pathophysiological processes, including sterol synthesis (3, 4), rheumatoid arthritis (5), fungal differentiation (6), cystic fibrosis (7, 8), and several neurodegenerative diseases (9). Accordingly, there is great impetus to understand the molecular mechanisms that mediate this broadly important route of protein degradation.

ERAD proceeds by the ubiquitin-proteasome pathway, by which an ER-localized substrate is covalently modified by the addition of multiple copies of 7.6-kDa ubiquitin to form a multiubiquitin chain that is recognized by the cytosolic 26S proteasome (10, 11). Ubiquitin is added to the substrate by the successive action of three enzymes. The E1 ubiquitin-activating enzyme uses ATP to covalently add ubiquitin to an E2 ubiquitin-conjugating (UBC) enzyme. Ubiquitin is then transferred from the charged E2 to the substrate or the growing ubiquitin chain by the action of an E3 ubiquitin ligase, resulting in a substrate-attached multiubiquitin chain that is recognized by the proteasome, leading to degradation of the ubiquitinated substrate. This is a skeletal picture; in most cases, ancillary factors participate in substrate recognition and transfer of the ubiquitinated substrate to the proteasome (12–14).

ERAD substrates are either sequestered in the lumen or embedded in the ER membrane with luminal portions. Thus, a critical step in the ERAD pathway involves transfer of the ERAD substrate to the cytosol for proteasomal degradation by a process referred to as retrotranslocation or dislocation (15). Retrotranslocation requires the hexameric AAA-ATPase called Cdc48p in yeast and p97 in mammals, and it is thought that a protein channel mediates the movement of substrates across the ER membrane. Channel candidates include the derlins (16, 17), the Sec61p anterograde channel (18, 19), or the multispanning domains of the ER ligases themselves (18–20).

The yeast HRD pathway mediates ERAD of numerous misfolded ER proteins and the physiologically regulated degradation of the Hmg2p isozyme of HMG-CoA reductase, an 8-transmembrane span (8-spanning) integral membrane protein critical for sterol synthesis (3). The integral membrane ER ligase Hrd1p, in conjunction with Hrd3p, is responsible for ubiquitination of Hmg2p. Efficient delivery of ubiquitinated Hmg2p to the proteasome requires the Cdc48p-Ufd1p-Npl4p

* This work was supported, in whole or in part, by National Institutes of Health Grant 5 R01 DK051996-15 (to R. Y. H.) with an additional Minority Supplement (to R. M. G.).

[S] The on-line version of this article (available at <http://www.jbc.org>) contains supplemental Table S1 and Fig. S1.

¹ To whom correspondence should be addressed: Section of Cell and Developmental Biology, Division of Biological Sciences, University of California, San Diego, 9500 Gilman Dr., La Jolla, CA 92093-0347. Tel.: 858-822-0511; Fax: 858-534-0555; E-mail: rhampton@ucsd.edu.

² The abbreviations used are: ER, endoplasmic reticulum; ERAD, endoplasmic reticulum-associated degradation; E1, ubiquitin-activating enzyme; HMG, 3-hydroxy-3-methylglutaryl; GFP, green fluorescent protein; HA, hemagglutinin; WT, wild type; AMP-PNP, adenosine 5'-(β,γ -imino)triphosphate; MOPS, 4-morpholinepropanesulfonic acid; IP, immunoprecipitation; GST, glutathione S-transferase; 8-spanning, 8-transmembrane span; E2, ubiquitin-conjugating enzyme; E3, ubiquitin-protein ligase.

complex presumably by promoting retrotranslocation of ER-embedded Hmg2p.

Due to the requirement for retrotranslocation in all ERAD pathways we have adapted our *in vitro* assay of Hrd1p-mediated ubiquitination of the normally degraded fusion Hmg2p-GFP to study this ER removal step in ERAD. We have reconstituted Hrd1p-mediated ubiquitination and retrotranslocation of Hmg2p-GFP *in vitro* (21, 22). We have now directly demonstrated that the entire 8-spanning Hmg2p-GFP protein is removed from the membrane by this process, remaining intact yet soluble after retrotranslocation. The dislocation of intact Hmg2p-GFP required both Cdc48p and hydrolysis of the β - γ bond of ATP. The Ubx2p adaptor protein functioned in a manner consistent with its proposed role in Cdc48p anchoring to the ER. Surprisingly, the Dsk2p/Rad23p proteasomal coupling factors were also required for retrotranslocation. Neither derlins nor Sec61p were implicated in Hmg2p-GFP retrotranslocation by our assay. Furthermore, an engineered substrate based on HMG-CoA reductase underwent ERAD in the complete absence of Hrd1p or Doa10p and *in vitro*, full-length retrotranslocation, both indicating that the large transmembrane domains of either of these ERAD E3 ligases were not required for membrane extraction. Taken together, these studies define a core set of proteins that can mediate recognition and retrotranslocation of the HRD substrate Hmg2p-GFP and will allow mechanistic analysis along all points of the ERAD pathway.

EXPERIMENTAL PROCEDURES

Strains and Media—All strains were derived from the S288C derivative genetic background and grown at 30 °C with aeration, as described previously (23). Yeast strains are listed in Table S1. Cultures used for assessing degradation by cycloheximide chase and microsome donor strains were logarithmically grown in minimum medium with 2% glucose and appropriate amino acid supplements ($A_{600} < 0.35$). Cytosol donor strains were grown in YPD medium to an A_{600} between 0.8 and 1.2. Standard yeast techniques used to integrate plasmids, prepare gene deletions, and incorporate mutant alleles are detailed in the supplemental material.

In Vitro Ubiquitination—*In vitro* reactions were prepared and analyzed as described previously (21, 22), and are delineated in detail in the supplemental material. Briefly, cytosols from strains overexpressing Ubc7p or an otherwise identical *ubc7* Δ null strain were prepared similarly to those from the Schekman laboratory (24). Cytosol strains were lysed by grinding under liquid nitrogen and ultracentrifuged for membrane removal. Typically, 1 mM ATP was added to cytosol; however, ATP was not added in AMP-PNP (Sigma) experiments, to allow choice of nucleotide during the two reaction phases. Protein concentration was measured using Bradford reagent. Cytosol concentrations were adjusted to 20–25 mg/ml for ubiquitination and retrotranslocation assays. Microsomes were prepared from *ubc7* Δ null yeast strain expressing 3HA-Hrd1p and Hmg2p-GFP from the *TDH3* promoter by bead lysis followed by membrane fractionation. The microsomal pellets were resuspended in the same buffer used to prepare cytosol. MG-132 (Sigma) was added to microsome and cytosol preparations except where indicated.

One *in vitro* ubiquitination reaction typically consisted of 10 μ l of microsome suspension and 12 μ l of cytosol. ATP (500 mM stock) was added to each reaction to a final concentration of 30 mM to initiate reaction, and the reaction was then incubated for 1 h at 30 °C. The assay was stopped by solubilization in 200 μ l of SUME (1% SDS, 8 M urea, 10 mM MOPS, pH 6.8, 10 mM EDTA) with protease inhibitors and 5 mM *N*-ethylmaleimide. Detergent immunoprecipitation buffer was added prior to incubation of rabbit polyclonal antiserum (anti-GFP, anti-loop and anti-Hrd1p antisera, prepared in collaboration with Scantibodies, Inc. (Santee, CA)) for immunoprecipitation (IP) of Hmg2p-GFP, Hrd1p, or Hmg1-Hrd1p. Overnight incubation with antiserum was followed with Protein A-Sepharose (GE Healthcare) incubation for 2 h at 4 °C. Protein A beads were washed twice, aspirated to dryness, resuspended in 2 \times urea sample buffer (2 \times USB: 8 M urea, 4% SDS, 10% β -mercaptoethanol, 125 mM Tris, pH 6.8), and incubated at 50 °C for 10 min. IPs were resolved by SDS-PAGE using 8% Tris-glycine gels, transferred to nitrocellulose, and immunoblotted with monoclonal antibodies anti-ubiquitin (Zymed Laboratories Inc., South San Francisco, CA), anti-GFP (BD Biosciences), or anti-HA (Covance, Princeton, NJ). Goat anti-mouse conjugated with horseradish peroxidase (Jackson ImmunoResearch, West Grove, PA) recognized primary antibodies. Western Lightning chemiluminescence reagents (PerkinElmer Life Sciences) were used for immunodetection.

In Vitro Retrotranslocation—Each *in vitro* retrotranslocation set of total, supernatant, and pellet fractions was typically derived from one 3 \times *in vitro* ubiquitination reaction. The reaction was run at 30 °C for 1 h and terminated by the addition of 1.5 μ l of 50 \times *N*-ethylmaleimide to a final concentration of 5 mM. One reaction equivalent (typically 24 μ l) was transferred to one tube designated as total (*T* in Figs. 1–8), and another reaction equivalent was transferred to a tube for centrifugation for 1 h at 25,000 \times *g* at 4 °C. The resulting supernatant (*S*) was carefully removed, and the resulting pellet (*P*) was resuspended in the same volume as the supernatant and total fractions. Each fraction was solubilized with SUME and immunoprecipitated and detected as described. The use of identical volumes allowed direct visual comparison of the immunoblotted proteins present in each fraction.

Nondetergent Immunoprecipitation—*In vitro* ubiquitination and retrotranslocation was carried out as described but using nondetergent IP buffer (15 mM Na_2HPO_4 , 150 mM NaCl, 10 mM EDTA) in the immunoprecipitation of the supernatant fraction. Either preimmune, anti-GFP, or anti-loop antiserum was added and incubated in IPs. After the addition and incubation of Protein A-Sepharose, protein-bound beads were washed extensively with nondetergent IP buffer. Immunoprecipitated Hmg2p-GFP was removed from beads by the addition of sample buffer, resolved by 8% SDS-PAGE gels, and immunoblotted as described.

Ubiquitin Stripping—Recombinant Usp2-cc, the catalytic core of the deubiquitinating enzyme Usp2p, was a generous gift from the Kopito laboratory (Stanford University) and prepared from a plasmid derived from Rohan Baker (Australian National University). *In vitro* ubiquitination and retrotranslocation was carried out as described except that leupeptin was not added to any of the buffers used in the preparation of cytosol and micro-

Hrd1p-dependent Retrotranslocation of Hmg-CoA Reductase

somes. Seven *in vitro* ubiquitination reactions were incubated for 1 h at 30 °C and then centrifuged at 25,000 × *g*. The supernatant fractions were pooled. Two reaction equivalents (50 μl) of supernatant received 5 μl of Usp2-cc (0.8–1.6 mg/ml) or buffer. The Usp2-cc reactions were incubated for 1 h in a 37 °C incubator. The reactions were stopped with SUME containing PIs and *N*-ethylmaleimide, and retrotranslocated substrate was immunoprecipitated in the same way as described. Half of each IP was used for detection of anti-ubiquitin, and the other half was used to detect Hmg2p-GFP with anti-GFP or Hmg1-Hrd1p with anti-HA antibodies.

Use of GST-Ubiquitin—*In vitro* reactions were modified by the addition of either GST-ubiquitin (Boston Biochem, Cambridge, MA) or ubiquitin (Sigma) to a final concentration of 20 μM in the reaction mix. Retrotranslocation and detection were carried out as in other reactions, using anti-ubiquitin or anti-GFP immunoblotting.

Cycloheximide Chase of Hmg1-Hrd1p—Preparation of whole cell lysates was previously described (25). Logarithmically growing cells were incubated with the protein synthesis inhibitor cycloheximide (50 μg/ml) for the indicated times and broken by bead lysis. Cell lysates were separated by SDS-PAGE, and the degradation substrate was detected with anti-HA antibodies.

Protease Protection Assay—Microsomes were prepared from the strain expressing the Hmg1-Hrd1p fusion used in the *in vitro* retrotranslocation assay for trypsin digestion, as previously described (26). The microsomes were resuspended in reaction buffer and incubated with 150 μg/ml trypsin (Sigma) for 0, 2, 8, and 32 min. An equal volume of 2× USB buffer was added to stop the reactions. The samples were then separated by 14% SDS-PAGE, and immunoblots were detected with anti-Myc 9E-10 antibody (hybridoma from ATCC (Manassas, VA)).

Flow Cytometry—Flow cytometry was carried out as previously described (27). Yeasts grown in minimum medium with 2% glucose and appropriate amino acids into log phase ($A_{600} < 0.2$) were incubated with cycloheximide (50 μg/ml) for the times indicated. The BD Biosciences FACSCalibur flow cytometer measured the individual fluorescence of 10,000 cells. CellQuest software was used to analyze the data and plotted fluorescence *versus* cell count histograms.

RESULTS

In these studies, we employed Hmg2p-GFP, in which the catalytic domain was replaced with GFP. This substrate underwent entirely normal, HRD pathway-dependent regulated degradation like its parent protein Hmg2p (27). Hrd1p-mediated ubiquitination of Hmg2p-GFP involves both membrane-bound and soluble proteins. The E2 Ubc7p is soluble, as are ubiquitin, the proteasome, the Cdc48p complex, and other coupling factors, such as Rad23p. Conversely, the E3 ligase, the substrate, and Cue1p, the required anchor for Ubc7p, are integral membrane proteins. Our *in vitro* assay uses two distinct strains as sources of ER membranes and cytosol that are mixed to initiate the *in vitro* reaction (21, 22). The microsome strain expresses epitope-tagged ligase 3HA-Hrd1p, substrate Hmg2p-GFP, Cue1p, and any other membrane-bound proteins required for the process. The microsome strain harbors a null mutation in *UBC7*, rendering Hmg2p-GFP in a nonubiquitinated state prior to assay initiation (28). The cytosol

strain is devoid of Hmg2p-GFP and expresses Ubc7p from the strong *TDH3* promoter to provide a pool of soluble E2, and other cytosolic proteins required for ERAD. These microsome and cytosol strains were modified to produce mutant and null strains presented in every subsequent *in vitro* experiment.

The reaction is started by mixing Ubc7p-containing cytosol with microsomes and ATP, followed by incubation at 30 °C. Ubiquitin transfer is measured by immunoprecipitation of Hmg2p-GFP, SDS-PAGE, and immunoblotting for Hmg2p-GFP itself or ubiquitin. The assay reaction as used in this work follows a number of biological criteria of specificity, including strict dependence on Hrd1p, lysine-6 of Hmg2p,³ and Ubc7p and its membrane anchor Cue1p (22).

Hrd1p is expressed from the *TDH3* promoter at levels sufficient to operate in the absence of a number of ERAD factors, including Hrd3p (see below), Usa1p,⁴ and Yos9p.⁵ The assay thus defines the minimal components sufficient for successful retrotranslocation, providing the best avenue for complete reconstitution. Hrd1p at this level causes sufficient ubiquitination of Hmg2p-GFP for the recovery and direct detection of the retrotranslocated substrate (see below), allowing analysis of the dislocated Hmg2p-GFP species and the partner molecules needed for solubilization of a multispreading membrane protein. A typical ubiquitination reaction is shown in Fig. 1A, demonstrating the dependence on Hrd1p.

To directly evaluate Hmg2p-GFP retrotranslocation, we fractionated the *in vitro* reaction mix to assess the amount of ubiquitinated Hmg2p-GFP present in the soluble phase. Identical volumes were withdrawn from a reaction mix after incubation (see “Experimental Procedures”). One was processed without fractionation to evaluate total ubiquitinated Hmg2p-GFP. The other was centrifuged at 25,000 × *g*. The supernatant was removed, and the membrane pellet was resuspended in reaction buffer to the same volume as the removed supernatant. All three equal volume samples were then analyzed for ubiquitinated Hmg2p-GFP. The results of this retrotranslocation assay are shown in Fig. 1B, as three immunoblotting lanes labeled *T* (total reaction mix), *S* (supernatant), and *P* (pellet). Each lane includes the ubiquitin immunoblot (for ubiquitinated Hmg2p-GFP) and the GFP blot for unmodified Hmg2p-GFP. A significant portion of the ubiquitinated Hmg2p-GFP is in the supernatant, consistent with retrotranslocation. Immunoprecipitation of the supernatant with preimmune serum (see Fig. 2B) resulted in no anti-ubiquitin immunoreactivity, indicating that the ubiquitin immunoreactivity was from Hrd1p-modified Hmg2p-GFP generated in the reaction. The appearance of ubiquitinated Hmg2p-GFP in the supernatant was time-dependent (Fig. S1). We found that the intensity of the signal for retrotranslocated protein was greater (compare *S* lanes in Fig. 1C) when proteasome inhibitor MG-132 was added, indicating that the 20S core protease activity was contributing to lessened signal, either due to *in vitro* degradation of a fraction of the substrate or due to proteasome-bound ubiquitin proteases that are sensitive to core protease inhi-

³ R. M. Garza and R. Y. Hampton, manuscript in preparation.

⁴ S. Carroll and R. Y. Hampton, manuscript in preparation.

⁵ S. Carroll and R. Y. Hampton, unpublished observation.

Hrd1p-dependent Retrotranslocation of Hmg-CoA Reductase

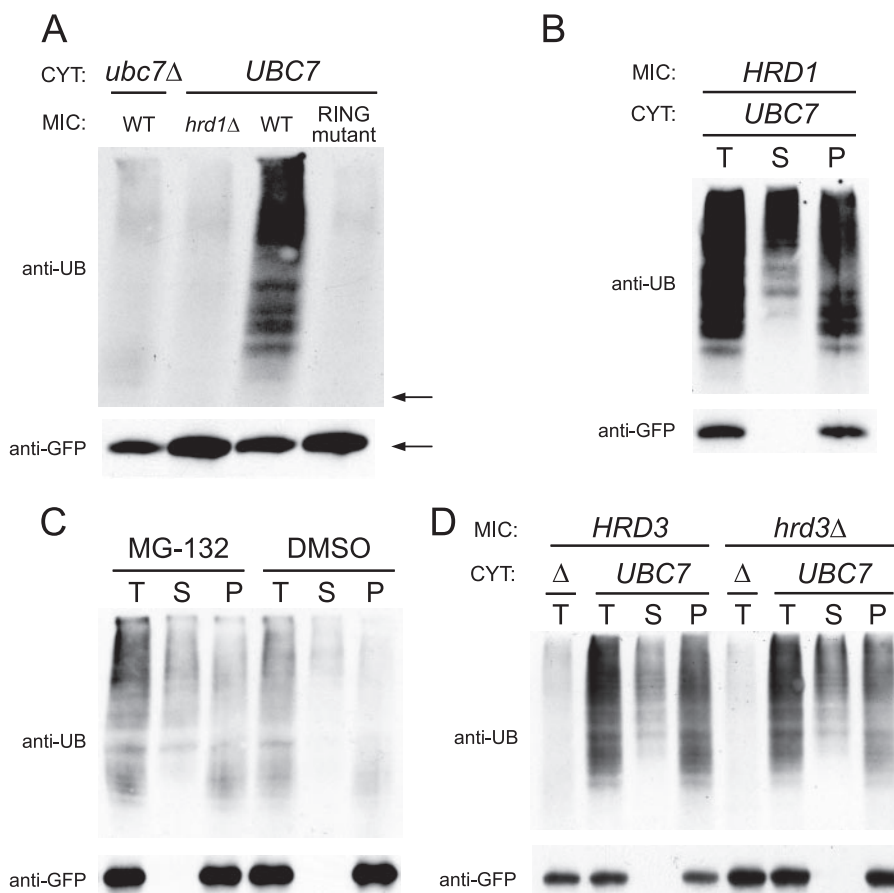


FIGURE 1. *In vitro* reconstitution of Hmg2p-GFP ubiquitination and retrotranslocation. *A*, Hmg2p-GFP *in vitro* ubiquitination required Ubc7p and Hrd1p. Microsomes (MIC) were prepared from strains expressing $TDH3_{PROM}$ -Hmg2p-GFP without Hrd1p (*hrd1*Δ), with $TDH3_{PROM}$ -Hrd1p (WT) or $TDH3_{PROM}$ -C399S-Hrd1p (*RING* mutant). Cytosol (CYT) was prepared from strains expressing $TDH3_{PROM}$ -Ubc7p (*UBC7*) or no Ubc7p (*ubc7*Δ). Reaction mixtures composed of microsomes and cytosols, as indicated, were incubated for 1 h, immunoprecipitated with anti-GFP, and immunoblotted for ubiquitin (*anti-UB*) or GFP (*anti-GFP*), as indicated. The arrows show mobility of unmodified Hmg2p-GFP. *B*, *in vitro* retrotranslocation of Hmg2p-GFP. Wild-type *in vitro* ubiquitination reactions were carried out as described in *A* but with 3 × volume (72 μl). Hmg2p-GFP was immunoprecipitated and immunoblotted from a 1 × (24-μl) aliquot of the nonfractionated mixture (*T*) or from the supernatant (*S*) and pellet (*P*) of an identical volume of the same reaction mixture that was centrifuged, as described. *C*, proteasome inhibitor increased the level of ubiquitinated Hmg2p-GFP. The ubiquitination and retrotranslocation assay was carried out in the absence or presence of proteasome inhibitor MG-132. *D*, *in vitro* Hmg2p-GFP ubiquitination and retrotranslocation was not dependent on Hrd3p. *In vitro* reactions were carried out with microsomes with Hrd3p (*HRD3*) or with no Hrd3p (*hrd3*Δ) incubated with cytosols with Ubc7p (*UBC7*) or with no Ubc7p (Δ).

bition.⁶ Thus, our *in vitro* ubiquitination and retrotranslocation assays included the proteasome inhibitor MG-132.

Membrane-embedded substrates and luminal substrates can be divided into two subpathways of ERAD, referred to as ERAD-M and ERAD-L, respectively. ERAD-L requires more components, including lectins/chaperones, such as Yos9p (29, 30), and traditional chaperones like Kar2p (31). These luminal proteins are not required for regulated degradation of Hmg2p. Furthermore, sufficient levels of Hrd1p will allow ERAD of both luminal and membrane-bound substrates in the absence of Hrd3p (30, 32). Because Hrd3p serves to anchor these luminal factors to the ER surface (30, 33), we tested if Hrd3p was required for the *in vitro* reactions described herein. The ubiquitination and retrotranslocation of Hmg2p-GFP in an *hrd3*Δ null strain was indistinguishable when compared with the nor-

⁶ D. Finley, personal communication.

mal *HRD3* strain (Fig. 1*D*). Thus, Hrd1p appears to play a central role in recognition and retrotranslocation of its substrate Hmg2p, as anticipated from its central role as defined by earlier genetic studies.

Retrotranslocation of the 8-spanning, ER-resident membrane protein, Hmg2p, is not energetically intuitive. We next performed several tests to evaluate if the appearance of ubiquitinated Hmg2p-GFP in the *S* fraction was *bona fide* retrotranslocation. Alternatively, the ubiquitin immunoreactivity that was immunoprecipitated with anti-GFP antibodies could be GFP-containing products cleaved from the transmembrane region in the microsomal membrane. We immunoprecipitated Hmg2p-GFP with antibodies against the first luminal loop (anti-loop) and the fourth luminal loop (data not shown), normally within the ER, and obtained results identical to those obtained with anti-GFP antibodies, indicating that both transmembrane domain and GFP epitopes are present in the soluble ubiquitinated substrate (Fig. 2*A*).

We next used serial immunoprecipitations with the anti-GFP and anti-luminal loop antisera to discern if the ubiquitinated Hmg2p-GFP in the soluble fraction was intact. If full-length ubiquitinated Hmg2p-GFP was moved to the cytosolic fraction in the assay, then either antibody should completely remove the ubiquitinated material from the soluble fraction. Three pairs (six identical samples total) of reaction supernatants were immunoprecipitated with either anti-GFP (two samples), anti-loop (two samples), or preimmune serum (two samples). The two identical supernatants from each pair were next reprecipitated with either anti-GFP or anti-loop antibodies. The precipitated material from all reactions was then subjected to ubiquitin immunoblotting, with the first round results in the *top panel* and the second round results in the *bottom panel* (Fig. 2*B*).

The serial IP experiment indicated that the retrotranslocated Hmg2p-GFP was intact. Immunoprecipitation of the soluble, ubiquitinated Hmg2p-GFP with either GFP or luminal antibodies completely cleared all of the ubiquitin immunoreactivity, resulting in no further pull-down of ubiquitinated Hmg2p-GFP with either antibody in the second IP. Conversely, reimmunoprecipitation of the supernatants from the preimmune pair with either antibody resulted in a

Hrd1p-dependent Retrotranslocation of Hmg-CoA Reductase

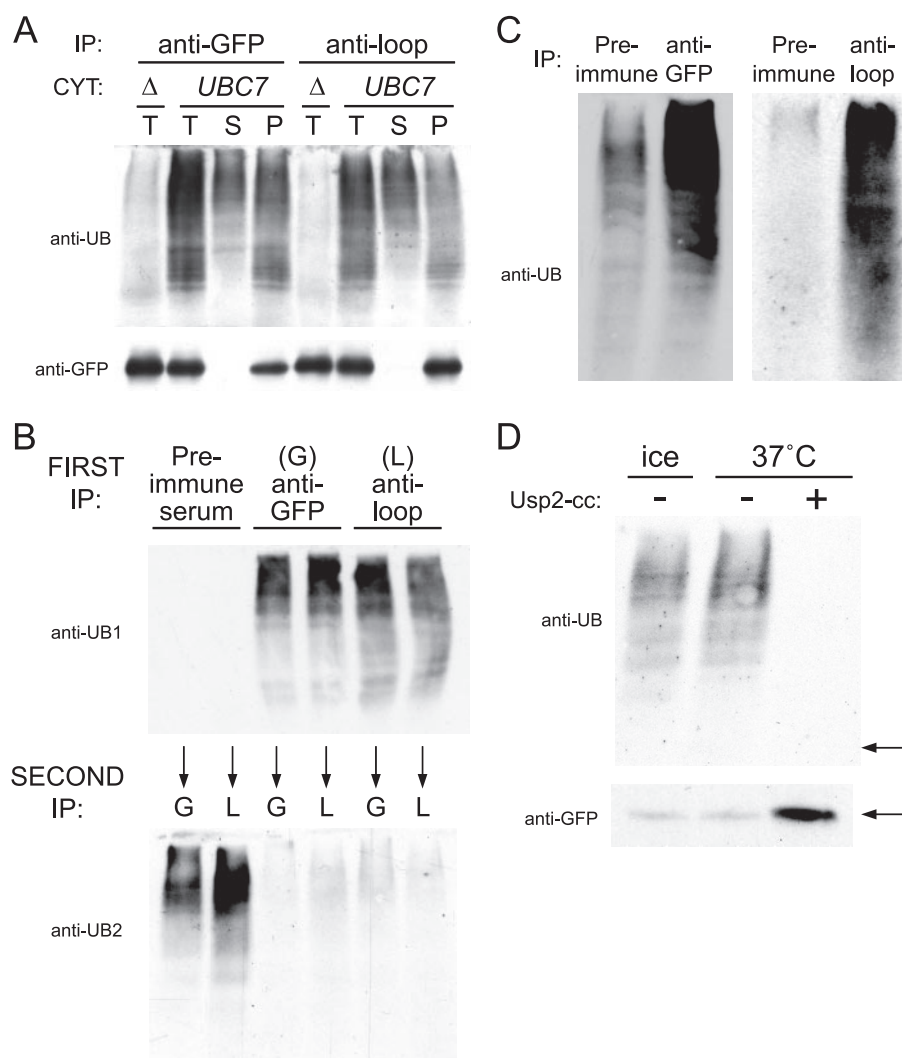


FIGURE 2. Retrotranslocation of full-length Hmg2p-GFP *in vitro*. *A*, Hmg2p-GFP retrotranslocation assays were carried out using either antiserum recognizing the cytosolic GFP (*anti-GFP*) or the first luminal loop (*anti-loop*) for the immunoprecipitation (*IP*) step. *B*, cytosolic and transmembrane epitopes of retrotranslocated Hmg2p-GFP could not be separately precipitated. Six supernatant fractions from six *in vitro* retrotranslocation reactions were subjected to serial immunoprecipitations. Pairs of supernatant fractions were first individually immunoprecipitated with preimmune, anti-GFP, or anti-loop antiserum, and the retrotranslocated Hmg2p-GFP was detected by anti-ubiquitin blotting (*anti-UB1*; top). The supernatant from each first immunoprecipitation was then subjected to a second round of immunoprecipitation with either anti-GFP (*G*) or anti-loop (*L*) antiserum as indicated and immunoblotted for ubiquitin (*anti-UB2*; bottom). *C*, nondetergent immunoprecipitation of *in vitro* retrotranslocated Hmg2p-GFP. Preimmune serum, anti-GFP, or anti-loop antiserum were used to immunoprecipitate retrotranslocated Hmg2p-GFP from two identical retrotranslocation assay supernatant fractions using a detergent-free IP buffer as described. *D*, ubiquitin protease treatment revealed that full-length Hmg2p-GFP was retrotranslocated *in vitro*. Identical supernatant fractions from retrotranslocation reactions were treated either with buffer or with the ubiquitin protease Usp2-cc for 1 h on ice or 37 °C, as described. The arrows point to mobility of full-length Hmg2p-GFP. *T*, total reaction mix; *S*, supernatant; *P*, pellet; *MIC*, microsomes; *CYT*, cytosol.

signal that was identical to either initial IP, showing that the supernatant samples from the first round of IP were competent for a second round and that the absence of signal in the second IPs (*middle* and *right* pairs) was due to a lack of any more ubiquitinated Hmg2p-GFP being present after either first round immunoprecipitation.

We did a separate experiment to confirm that the intact, ubiquitinated Hmg2p-GFP had been solubilized, by running the immunoprecipitation of the cytosolic *S* fraction in the absence of normally employed detergent (Fig. 2*C*). Parallel samples of the supernatant fraction were subjected to detergent-free immunoprecipitation with either preimmune serum

(*left, pre-immune*) or anti-GFP (*left, anti-GFP*). Similar results were obtained doing the same experiment with anti-loop antibodies (*right*). These data show that intact, full-length Hmg2p-GFP is present in the cytoplasmic fraction as a soluble protein, presumably in a complex with factors that mediate retrotranslocation.

The above experiments all indicate that intact, ubiquitinated Hmg2p-GFP is moved to the soluble fraction *in vitro*. To directly test if full-length Hmg2p-GFP was retrotranslocated, we used the recombinant catalytic core of the ubiquitin protease *USP2* (*Usp2-cc*) that efficiently strips ubiquitin from multiubiquitin chains on substrates (34), allowing us to directly examine the retrotranslocated material by GFP immunoblotting. Before immunoprecipitating the retrotranslocated, ubiquitinated protein, we divided the sample into three aliquots. One was incubated with buffer on ice, and the other two were incubated at 37 °C with either buffer or *Usp2-cc* (Fig. 2*D*). The *upper panel* shows an anti-ubiquitin blot of the sample and demonstrates the effect of the *Usp2-cc*. The *lower panel* shows the same sample immunoblotted with anti-GFP antibodies. Without ubiquitin stripping, there is little detectable GFP, whereas in the stripped sample, the GFP immunoreactivity appears at the molecular weight of Hmg2p-GFP (*arrow*). Importantly, only the mobility of full-length Hmg2p-GFP increased after *Usp2-cc* treatment. This experiment directly demonstrated that intact Hmg2p-GFP was being moved to the cytosol as a multiubiquitinated protein. We noticed that a band of

Hmg2p-GFP immunoreactivity was seen in the “unstripped” *S* fraction at varying intensities between experiments, which was not dependent on ubiquitination or the factors needed for retrotranslocation, and may be caused by some fragmentation of the ER. This background signal was not present when ubiquitin was used to detect the retrotranslocated material, and thus we used this method of detection. Nevertheless, it was important to directly demonstrate that Hmg2p-GFP is moved in its entirety to the soluble fraction.

A unifying feature of many ERAD pathways is the proposed role of the hexameric AAA-ATPase Cdc48p (p97 in mammals) in retrotranslocation (12, 35), along with its binding partners Ufd1p and

Hrd1p-dependent Retrotranslocation of Hmg-CoA Reductase

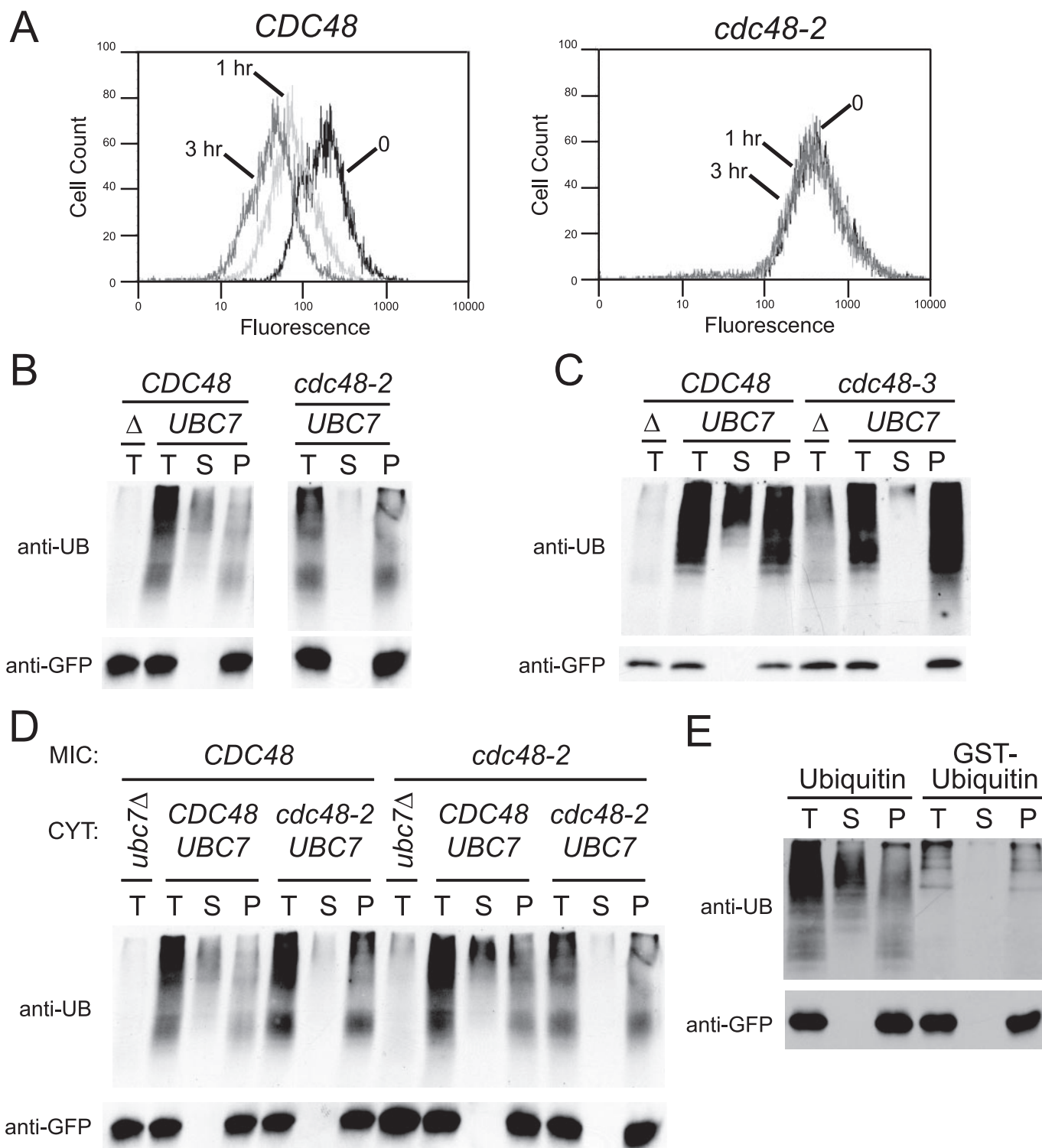


FIGURE 3. Role of Cdc48p in Hmg2p-GFP retrotranslocation. *A*, *in vivo* Hmg2p-GFP degradation was blocked by the *cdc48-2* mutant. WT (*CDC48*) and *cdc48-2* strains expressing Hmg2p-GFP were subjected to a cycloheximide chase and flow cytometry at the indicated times to evaluate Hmg2p-GFP levels. The experiment was done at 30 °C, a permissive temperature for this allele. Histograms of 10,000 cells are shown, with the number of cells versus GFP fluorescence. *B*, *in vitro* retrotranslocation of Hmg2p-GFP required Cdc48p. *In vitro* reactions were carried out in which both components were derived from either WT (*CDC48*) or *cdc48-2* strains (these panels were extracted from the more elaborate panel *D*). *C*, same experiment using reaction mixtures from WT or *cdc48-3* strains. *D*, strong requirement for cytosolic Cdc48p in retrotranslocation. The indicated combinations of WT or *cdc48-2* reaction components (microsomes (MIC) and cytosol (CYT)) were mixed, as indicated, to evaluate relative contribution to Hmg2p-GFP retrotranslocation. *E*, *in vitro* Hmg2p-GFP ubiquitination with GST-ubiquitin does not support Hmg2p-GFP retrotranslocation. Exogenous ubiquitin or GST-ubiquitin was added to the *in vitro* retrotranslocation assay, and anti-ubiquitin immunoblotting was used for detection of modified Hmg2-GFP. Lanes labeled Δ and *ubc7* Δ indicate reactions carried out with *ubc7* Δ cytosol and specified microsomes in *B–E*. T, total reaction mix; S, supernatant; P, pellet.

Hrd1p-dependent Retrotranslocation of Hmg-CoA Reductase

Npl4p (35, 36). Hmg2p is strongly stabilized by mutations in the Cdc48p complex, with a block that occurs after ubiquitination (12). We first confirmed that the *cdc48-2* allele shows a strong *in vivo* block in Hmg2p-GFP degradation, even at the permissive temperature of 30 °C (Fig. 3A). Then we tested the effect of this allele in our *in vitro* assay. When both microsome and cytosol strains were *cdc48-2*, ubiquitination occurred, but there was a nearly complete block in release of ubiquitinated Hmg2p-GFP into the cytoplasmic S fraction (Fig. 3B). Similar results were obtained using the *cdc48-3* allele (Fig. 3C).

The Cdc48p complex is found both in the microsome fraction and in the cytoplasmic pool (37), and some of the complex is bound to Hrd1p (30, 33, 38). Thus, we wondered whether membrane-bound or soluble Cdc48p provided the activity for retrotranslocation. We prepared microsomes and cytosol from strains with either normal *CDC48* or the *cdc48-2* allele and ran the retrotranslocation assay with the various combinations of mutant or wild-type material, as indicated (Fig. 3D; the *first four lanes* and the *last three lanes* of D are the same as shown in B). It was clear that the cytosol alone contributes the majority of the needed Cdc48p activity. This implies that soluble Cdc48p complexes are recruited from the aqueous medium for their role in retrotranslocation.

The Cdc48p complex has binding sites for ubiquitin, located both on Ufd1p and Cdc48p itself (36, 39). The importance of these sites has been demonstrated for the case of US11-mediated major histocompatibility complex I retrotranslocation, since p97-mediated retrotranslocation does not occur when a GST-ubiquitin fusion is used instead of native ubiquitin. Similarly, Hmg2p-GFP retrotranslocation was dependent on native ubiquitin. Use of the N-terminal GST-ubiquitin fusion allowed *in vitro* ubiquitination to proceed, producing large conjugates in the reaction mix (Fig. 3E). However, there was little or no movement of the GST-ubiquitin-derivatized Hmg2p-GFP to the cytosol, underscoring the importance of the ubiquitin molecule in the retrotranslocation process. Interestingly, a similar experiment with K6W ubiquitin, which blocks proteasomal degradation (40), did not inhibit the retrotranslocation assay (data not shown).

Dislocation of an 8-spanning integral membrane protein would require significant energy. Hexameric Cdc48p is a member of the large AAA-ATPase family, and this activity is thought to drive retrotranslocation. We wanted to directly examine this question with our assay. To specifically test the role of ATP in retrotranslocation, we capitalized on the differing use of ATP by the ubiquitin E1 or the AAA-ATPase domains of Cdc48p. Ubiquitin addition to the E1 is driven by hydrolysis of the α - β phosphodiester bond, whereas the AAA-ATPases hydrolyze the β - γ bond (41). In numerous cases, the β - γ imido analog of ATP, called AMP-PNP, with a normal α - β bond but a non-hydrolyzable phosphodiimido linkage to the γ -phosphate position, will drive ubiquitination (42) but not reactions that depend on β - γ hydrolysis. We employed AMP-PNP to test for a role of ATP in retrotranslocation separate from its known involvement in ubiquitination. The direct approach of simply adding AMP-PNP to the retrotranslocation assay rather than normal ATP was not an effective way to ask this question. In our *in vitro* assay, although AMP-PNP did support Hmg2p-GFP ubiq-

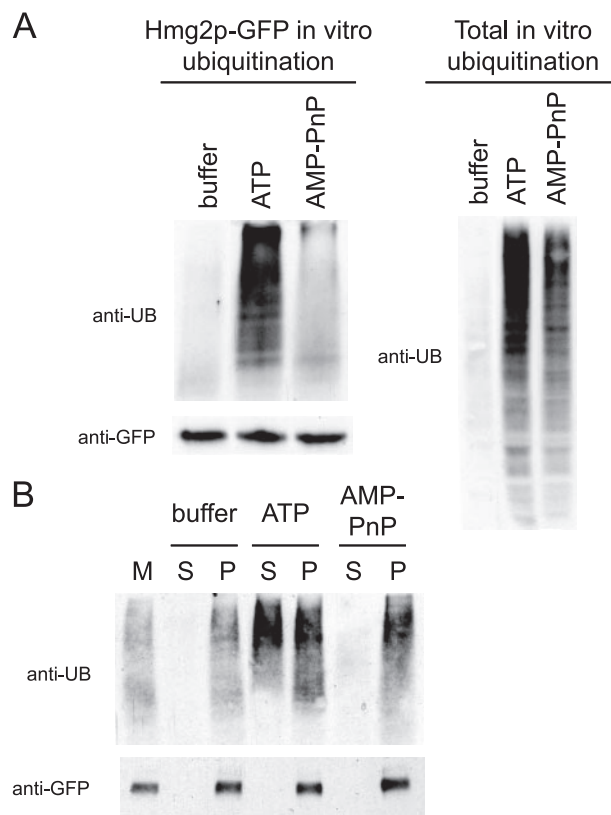


FIGURE 4. ATP dependence of Hmg2p-GFP retrotranslocation. A, *in vitro* Hmg2p-GFP ubiquitination was compromised in the presence of AMP-PNP. Buffer, ATP (30 mM), or AMP-PNP (30 mM) was added to *in vitro* ubiquitination reactions, as indicated. Hmg2p-GFP was immunoprecipitated, and ubiquitinated Hmg2p-GFP was detected (*Hmg2p-GFP in vitro ubiquitination*). These concentrations of the nucleotide supported similar levels of total *in vitro* ubiquitination, evaluated by direct ubiquitin immunoblotting of a 1- μ l sample of whole reaction mixtures (*Total in vitro ubiquitination*). B, direct ATP requirement for *in vitro* Hmg2p-GFP retrotranslocation. Five *in vitro* ubiquitination reactions were carried out with *cdc48-2* microsomes and *cdc48-2* UBC7 cytosol to minimize retrotranslocation. Following the 1-h incubation, the reaction mixes were pooled and fractionated into pellet and supernatant by centrifugation. The supernatant was discarded, and the prereacted microsomes were resuspended and then incubated with *CDC48 ubc7 Δ* cytosol in the presence of buffer, ATP (30 mM), or AMP-PNP (30 mM), for an additional 1 h to assay retrotranslocation. The supernatant (S) and pellet (P) fractions were separated by centrifugation, and Hmg2p-GFP was immunoprecipitated from each fraction with anti-GFP antiserum. M, the starting Hmg2p-GFP level of ubiquitination in the membrane fraction prior to the retrotranslocation phase of the experiment. Note that AMP-PNP supported further UBC7-independent ubiquitination but no retrotranslocation.

uitination, the reaction did not proceed to nearly the same extent as those run with ATP, prohibiting direct comparison with the two nucleotides (Fig. 4A, left). This appeared to have some specificity for the HRD pathway, since AMP-PNP did support total lysate *in vitro* ubiquitination, evaluated by ubiquitin immunoblotting of the nonimmunoprecipitated proteins in the total reaction mix (Fig. 4A, total *in vitro* ubiquitination; right).

This requirement for the β - γ ATP bond in Hmg2p-GFP ubiquitination required a more complex procedure to test an ATP requirement in retrotranslocation. We first ran a ubiquitination phase of the assay with ATP to ensure sufficient Hmg2p-GFP ubiquitination and then a retrotranslocation phase with either ATP or AMP-PNP to test for ATP dependence of retrotranslocation of the ubiquitinated Hmg2p-GFP. The major contribution of soluble Cdc48p to Hmg2p-GFP retrotranslocat-

Hrd1p-dependent Retrotranslocation of HMG-CoA Reductase

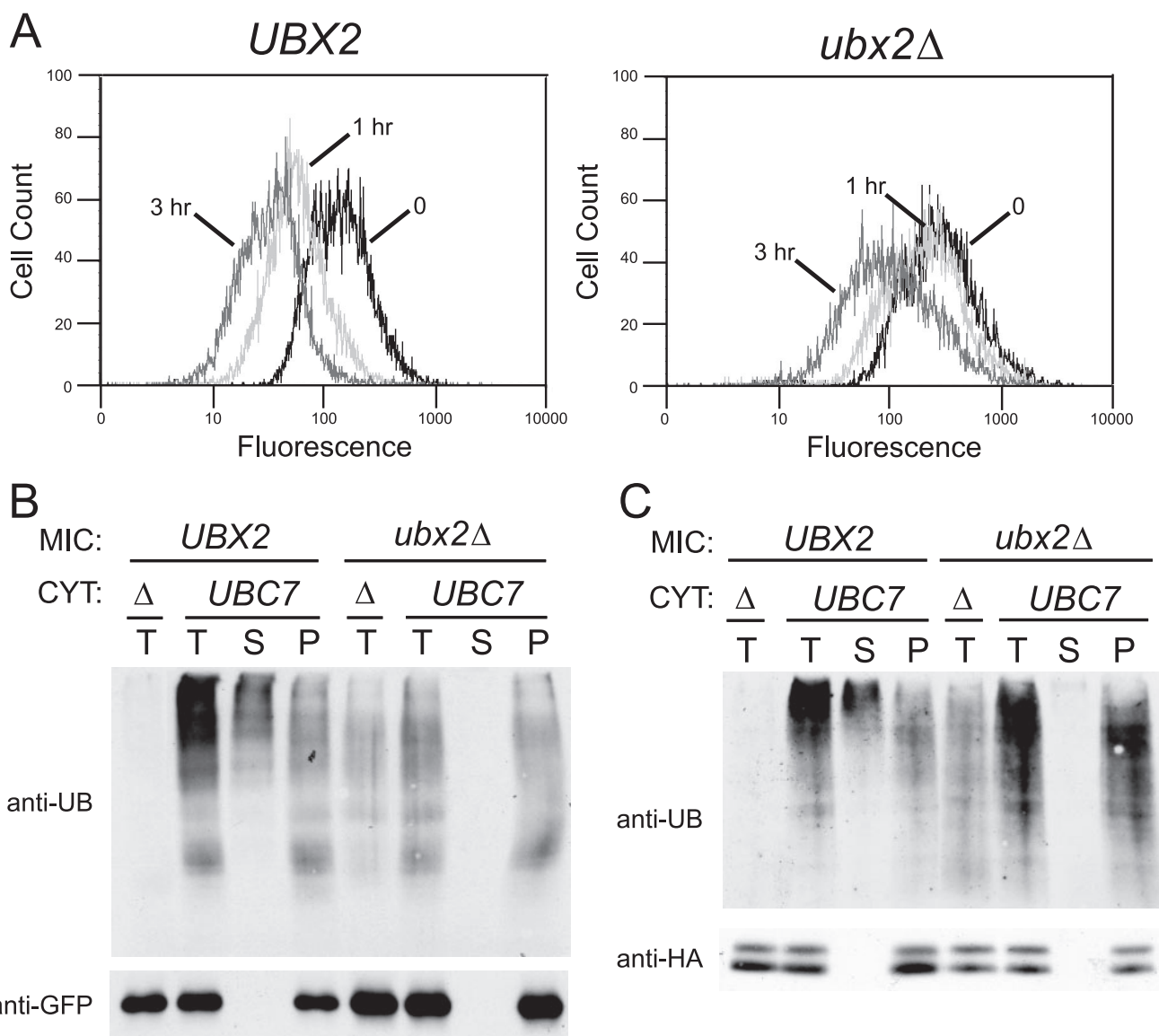


FIGURE 5. Ubx2p was necessary for retrotranslocation. *A*, *in vivo* Hmg2p-GFP degradation in WT or *ubx2Δ* strains. Hmg2p-GFP degradation was assayed by the addition of cycloheximide to WT (*UBX2*) or *ubx2Δ* strains and followed by flow cytometry (10,000 cells) to evaluate cellular Hmg2p-GFP, as in Fig. 3. *B* and *C*, *in vitro* retrotranslocation of Hmg2p-GFP and Hrd1p was blocked in the absence of Ubx2p. Hmg2p-GFP (*B*) and Hrd1p (*C*) retrotranslocation were evaluated in WT (*UBX2*) and *ubx2Δ* microsomes incubated with *ubc7Δ* (Δ) or *UBC7* cytosol in the *in vitro* assay. Hrd1p was immunoprecipitated with polyclonal anti-Hrd1p antiserum. *T*, total reaction mix; *S*, supernatant; *P*, pellet; *MIC*, microsomes; *CYT*, cytosol.

tion allowed us to accomplish this separation. This was done by running the “ubiquitination phase” with *cdc48-2* microsomes and *cdc48-2* cytosol with ATP present. After a reaction period, we recovered the *cdc48-2 ubc7Δ* microsomes from the reaction by centrifugation and initiated the second “retrotranslocation phase” by adding *CDC48* cytosol from a *ubc7Δ* null to those microsomes. This *CDC48 ubc7Δ* cytosol was supplemented with either ATP or AMP-PNP, along with a control in which buffer was added to the microsomes. The reaction mixes were then fractionated to evaluate soluble and membrane-bound ubiquitinated Hmg2p-GFP (Fig. 4*B*). The reaction with AMP-PNP did not support retrotranslocation, but did allow continued ubiquitination when compared with the buffer control. In contrast, the cytosol with ATP did retrotranslocate Hmg2p-GFP and also supported further ubiquitination. Clearly, a β - γ ATP bond is needed for Cdc48p-dependent retrotranslocation.

How does the Cdc48p complex engage the HRD complex at the ER surface? It has been proposed that the ER membrane protein Ubx2p serves as an ER-localizing “receptor” or docking site for the Cdc48p complex (43–45). However, *in vivo*, loss of Ubx2p only partially blocks ERAD. This is clear in previous reports (43–45), and is demonstrated in Fig. 5*A*, with Hmg2p-GFP cycloheximide chase. Thus, there may be other ways for Cdc48p to get to the ERAD process *in vivo*, since a complete null of the Ubx2p “receptor” has a less strong effect on Hmg2p-GFP ERAD than the partially functioning hypomorph of *cdc48-2* (Fig. 3*A*). Furthermore, *ubx2Δ* null strains have numerous physiological alterations, such as a highly elevated unfolded protein response⁷ that may obscure studies of the molecular

⁷ B. K. Sato and R. Y. Hampton, unpublished observations.

Hrd1p-dependent Retrotranslocation of Hmg-CoA Reductase

actions of Ubx2p *in vivo*. Thus, we used the *in vitro* assay to directly test the role of this adaptor in Cdc48p-dependent retrotranslocation.

When the assay was run with *ubx2Δ* cells, retrotranslocation was completely abrogated, as shown by the lack of immunoreactivity in the soluble fraction (Fig. 5B). Furthermore, cytosol from a wild-type *UBX2* strain did not allow retrotranslocation from membranes prepared from a *ubx2Δ* null strain (data not shown). However, *ubx2Δ* microsomes also showed unexpected ubiquitination of Hmg2p-GFP in the absence of added Ubc7p. This Hrd1p-dependent ubiquitination of Hmg2p-GFP is present in the microsomes before the reaction is initiated and was observed when Hmg2p-GFP was directly immunoprecipitated from lysates of the *ubx2Δ ubc7Δ* double null microsome strain (data not shown). This *ubx2Δ*-caused "preubiquitination" was highly reproducible and implies that Ubx2p may have roles at other positions in the ERAD pathway, at least of Hmg2p-GFP. At present, we do not know how this process occurs.

We confirmed the generality of the requirement for Ubx2p in retrotranslocation by examining Hrd1p itself as a substrate. Hrd1p levels were sufficiently elevated to allow *in vitro* Hrd1p self-ubiquitination, mediated by the RING domain of Hrd1p (28). *In vitro* Hrd1p retrotranslocation occurred and was also dependent on Ubx2p (Fig. 5C). The block to retrotranslocation caused by *ubx2Δ* was strong with either Hmg2p-GFP or Hrd1p.

A number of studies have implicated the set of adaptor proteins Dsk2p and Rad23p that facilitate transfer of ubiquitinated ERAD substrates to the proteasome. These adaptors have both ubiquitin-binding Uba motifs and proteasome-binding Ubl motifs (46, 47). Although these adaptors are proposed to function in proteasome delivery, they in fact had a strong role in Hmg2p-GFP retrotranslocation (Fig. 6A).

Both Rad23p and Dsk2p are soluble proteins (48) and might be expected to be supplied from the cytosolic fraction. However, the actions of the pair were more complex and indicated that they may have multiple roles in the ERAD pathway. It appeared that Rad23p/Dsk2p functioned both in the extent of Hmg2p-GFP ubiquitination and retrotranslocation (Fig. 6B, compare *first* and *third sets*). Furthermore, these two actions were to a large extent separable between the cytosolic and membrane fractions used in the assay. When the *rad23Δ dsk2Δ* double null was present in both the microsomes and cytosol, retrotranslocation was severely curtailed, and the extent of Hmg2p-GFP ubiquitination (compare total reaction lanes from all-WT and all-null sets) was lessened. Use of individual fractions with or without Rad23p and Dsk2p showed that the retrotranslocation was significantly restored (but not completely) by the presence of these factors solely in the microsome strains (Fig. 6B, *second set, MIC: RAD23 DSK2* with *CYT: rΔdΔ UBC7*), without alleviation of the lessened extent of ubiquitination. Conversely, the presence of Rad23p and Dsk2p in only the cytosol fraction allowed for ubiquitination of the higher molecular weight conjugates, but retrotranslocation was still poor (Fig. 6B, *fourth set, MIC: rad23Δ dsk2Δ* with *CYT: RD UBC7*). Thus, it is likely that Rad23p and Dsk2p have functions at a number of points along the ERAD pathway and distinct functions at the ER surface and in the cytosolic fractions.

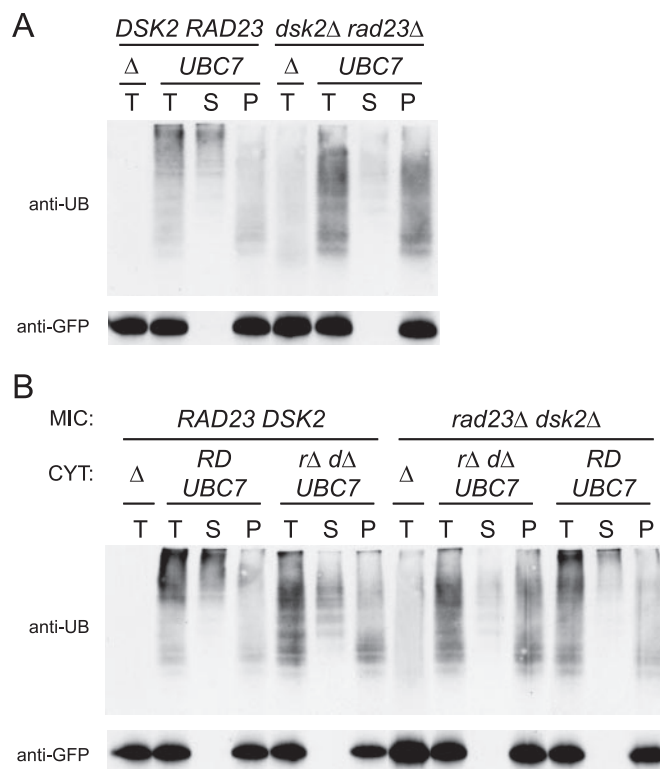


FIGURE 6. Rad23p and Dsk2p were required for *in vitro* Hmg2p-GFP retrotranslocation. A, Hmg2p-GFP *in vitro* retrotranslocation was evaluated in reaction mixtures prepared from WT (*RAD23 DSK2*) or *rad23Δ dsk2Δ* strains. WT cytosol was reacted with WT microsomes, and double null cytosol was incubated with double null microsomes. B, role of cytosolic or microsomal Rad23p and Dsk2p in Hmg2p-GFP retrotranslocation. Reaction mixtures were composed of WT (*RAD23 DSK2*) or mutant (*rad23Δ dsk2Δ*) microsomes mixed with WT (*RD UBC7*) or mutant (*rΔdΔ UBC7*) cytosol as indicated. Cytosol lacking Ubc7p (Δ) was also reacted with the specified microsomes in A and B. T, total reaction mix; S, supernatant; P, pellet; MIC, microsomes; CYT, cytosol.

It is widely thought that a pore or channel is required for the removal of ERAD substrates. The most often proposed candidates for such a pore include members of the derlin family (49, 50), or the anterograde pore Sec61p. Yeast expresses two derlins, the original Der1p protein and its homologue Dfm1p that has demonstrable Cdc48p-binding activity (51), but the double null has no *in vivo* defect on Hmg2p-GFP ERAD. *In vivo* analysis of the role of Sec61p in ERAD or retrotranslocation has been challenging, because hypomorphs of this essential gene have a variety of effects on ER processes. Nevertheless, a *sec61-2* mutant has small but reproducible deficiencies in ERAD of Hmg2p-GFP. We wondered if the highly sensitive retrotranslocation assay would reveal any roles for these factors that are harder to observe *in vivo*, as appears to be the case for the *ubx2Δ* null above. We tested membranes from a *der1Δ dfm1Δ* double null strain in the retrotranslocation assay (Fig. 7A) and membranes from the *sec61-2* strain (Fig. 7B). As a control, we included the *ubx2Δ* null that had blocked Hmg2p-GFP retrotranslocation. In no case was there any effect of these mutants on *in vitro* retrotranslocation of Hmg2p-GFP. Furthermore, assay of *sec61-2* function in microsomes at the nonpermissive temperature (37 °C) had no effect on *in vitro* retrotranslocation (data not shown).

These results led us to wonder if Hrd1p itself was providing channel function in addition to its role as the E3 ligase. Hrd1p

Hrd1p-dependent Retrotranslocation of HMG-CoA Reductase

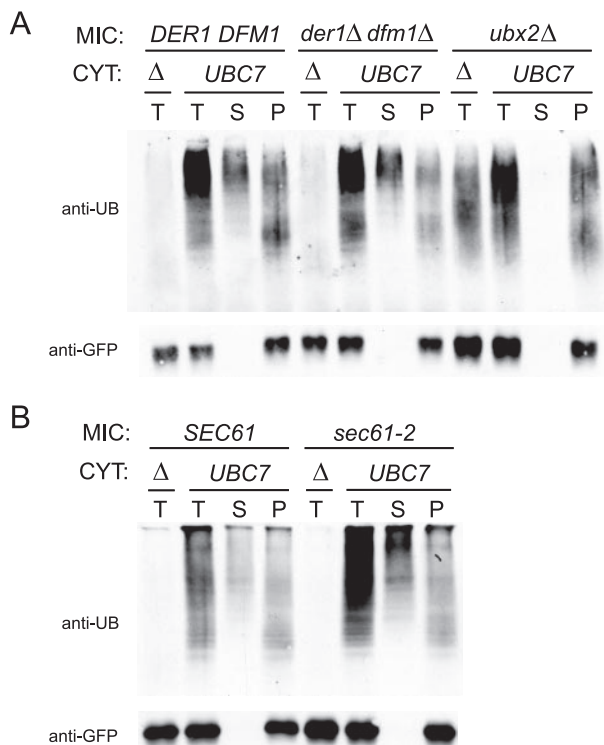


FIGURE 7. Direct evaluation of channel candidates derlins Der1p/Dfm1p or Sec61p in Hmg2p-GFP retrotranslocation. *In vitro* Hmg2p-GFP retrotranslocation reactions consisting of WT derlins (*DER1 DFM1*) or *der1Δ dfm1Δ* microsomes in *A* and the anterograde channel *SEC61* or *sec61-2* microsomes in *B* were reacted with *ubc7Δ* (Δ) or *UBC7* cytosol. *T*, total reaction mix; *S*, supernatant; *P*, pellet; *MIC*, microsomes; *CYT*, cytosol.

has a multispanning membrane domain N-terminal to its RING ligase domain, which would allow simultaneous coupling of protein dislocation and ubiquitination.

The simple experiment of removing Hrd1p to test its role in retrotranslocation was not feasible, because it is also necessary for Hmg2p ubiquitination, which is a prerequisite for retrotranslocation. To separate the Hrd1p ligase function from other possible activities, we devised a “self-destructive” substrate that employs the Hrd1p RING domain in the absence of its transmembrane region. We prepared a coding region that expresses the C-terminal Hrd1p cytosolic RING domain fused to the N-terminal transmembrane domain of the normally stable Hmg1p HMG-CoA reductase isozyme; the resulting fusion is called Hmg1-Hrd1p (Fig. 8A). The Hmg1p transmembrane region had an epitope tag inserted in the first luminal domain, in the same position used to study the *in vivo* and *in vitro* folding state of Hmg2p by limited proteolysis in earlier work (26). We confirmed that the luminal Myc tag showed the expected protection in limited proteolysis (Fig. 8B), and the HA cytosolic tag disappeared with trypsin addition (not shown), consistent with the fusion being correctly inserted in the ER membrane. *In vivo*, Hmg1-Hrd1p behaved in all ways like a HRD pathway substrate but did not require the presence of Hrd1p due to its *cis* RING domain. Hmg1-Hrd1p degradation was very rapid and strongly dependent on both Ubc7p (Fig. 8C) and its intact RING domain (not shown). A lighter exposure of the *ubc7Δ* lanes is shown below the original lanes to demonstrate the slower degradation in this strain. Rapid Hmg1-Hrd1p degradation occurred in an

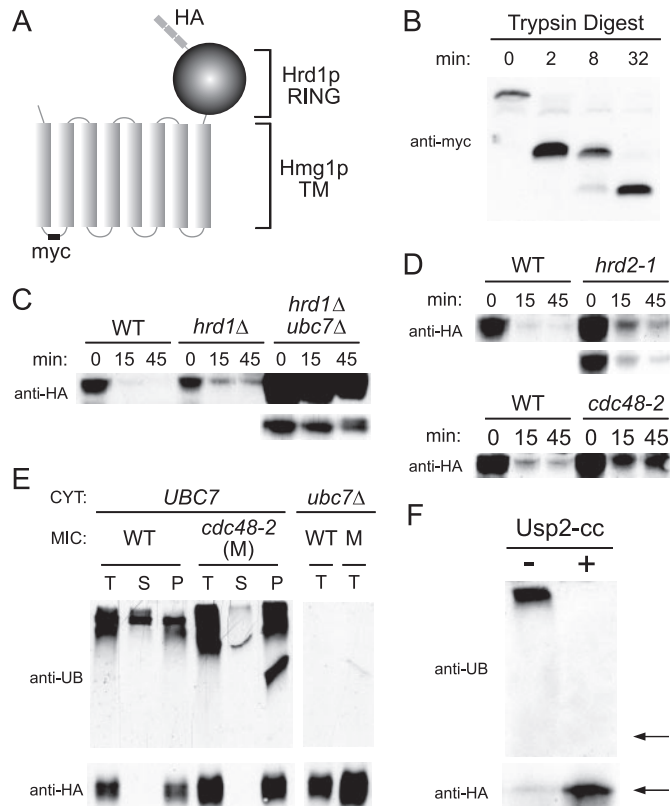


FIGURE 8. The self-destructive substrate, Hmg1-Hrd1p. *A*, depiction of fusion protein Hmg1-Hrd1p. The transmembrane Hmg1p domain has a luminal Myc epitope, and the cytosolic domain of Hrd1p has three HA epitopes. *B*, Hmg1-Hrd1p fusion protein was correctly inserted into ER membrane. Microsomes prepared from strain expressing Hmg1-Hrd1p were digested with trypsin for the indicated times and immunoblotted with anti-Myc. *C* and *D*, degradation behavior of Hmg1-Hrd1p was assayed by cycloheximide chase. *C*, degradation of Hmg1-Hrd1p was dependent on Ubc7p. *D*, degradation of Hmg1-Hrd1p was dependent on *cdc48-2* and *hrd2-1*. The *ubc7Δ* and *hrd2-1* lanes include lower intensity exposures to facilitate comparison with the wild-type lanes. *E*, *in vitro* retrotranslocation of Hmg1-Hrd1p fusion was dependent on Cdc48p. Reactions with Ubc7p from WT (*CDC48 UBC7*) or *cdc48-2* (*cdc48-2 UBC7*) and without Ubc7p (Δ) were carried out with *hrd1Δ* microsomal strains *CDC48* (WT) or *cdc48-2* expressing Hmg1-Hrd1p from the *TDH3* promoter. Fusion protein was immunoprecipitated with anti-Hrd1p antiserum and immunoblotted with anti-ubiquitin and anti-HA antibodies. Anti-ubiquitin (*anti-UB*) panels were derived from the same gel, as were *anti-HA* panels. Extraneous lanes were removed. *M*, mutant *cdc48-2*. *F*, Usp2-cc ubiquitin protease treatment revealed that full-length Hmg1-Hrd1p was retrotranslocated *in vitro*. Supernatant fractions from *in vitro* reactions were treated either with buffer or with ubiquitin-specific protease Usp2-cc. The arrows point to mobility of unmodified Hmg1-Hrd1p. *T*, total reaction mix; *S*, supernatant; *P*, pellet; *MIC*, microsomes; *CYT*, cytosol.

hrd1Δ null mutant (Fig. 8C) and in the *hrd1Δ doa10Δ* double mutant (data not shown). Hmg1-Hrd1p degradation was also slowed by mutations *cdc48-2* or the proteasomal *RPN1* hypomorph *hrd2-1* (Fig. 8D). Again, a lighter exposure of the *hrd2-1* mutant at a similar initial intensity to the wild-type is included to facilitate comparison. The rapid, Cdc48p-dependent degradation of Hmg1-Hrd1p implied that the autonomously degrading fusion protein undergoes retrotranslocation. We tested this directly *in vitro*. Hmg1-Hrd1p underwent Ubc7p-dependent *in vitro* ubiquitination and showed the expected movement to the soluble supernatant fraction (Fig. 8E). Furthermore, Hmg1-Hrd1p retrotranslocated from microsomes derived from a *hrd1Δ* null strain. Hmg1-Hrd1p retrotranslocation was partially blocked in an assay run with both cytosol and supernatant

Hrd1p-dependent Retrotranslocation of Hmg-CoA Reductase

from the *cdc48-2* mutant (Fig. 8E). Finally, use of the Usp2-cc ubiquitin protease demonstrated that full-length Hmg1-Hrd1p was being retrotranslocated (Fig. 8F). Thus, Cdc48p-mediated retrotranslocation of this HRD pathway substrate can occur in the complete absence of the Hrd1p transmembrane domain.

DISCUSSION

In this study, we have successfully reconstituted Hrd1p-dependent retrotranslocation of a multispreading membrane substrate of the HRD pathway, Hmg2p-GFP. By multiple criteria, we have shown the ubiquitinated, full-length Hmg2p-GFP is moved to the supernatant fraction. The ability to observe this process with Hmg2p-GFP both defines the capacity of this transfer mechanism and allows its intimate mechanistic study in ways that are not possible using intact cells.

In our approach, we have used sufficient Hrd1p levels to drive ubiquitination of Hmg2p-GFP without need for Hrd3p or Usa1p. Thus, we are examining the minimal requirements for *in vitro* ubiquitination and retrotranslocation. Importantly, *in vitro* ERAD of Hmg2p-GFP by this method has all of the features of *in vivo* Hmg2p-GFP degradation.³ Ubc7p and its anchor Cue1p are required, as is the critical lysine 6 of Hmg2p-GFP (52, 53). Furthermore, Hrd1p-dependent ubiquitination of Hmg2p-GFP is specifically blocked by chemical chaperones as is *in vivo* degradation of this substrate (52). These studies also reinforce the idea that Hrd1p is a central organizer of ERAD, consistent with multiple observations that Hrd1p alone can drive ERAD of membrane-anchored substrates (32, 54).⁴

A recent, elegant study of ERAD using radioiodinated ubiquitin provides a distinct approach for the biochemical study of these processes (55). The radiochemical analysis therein is more sensitive and somewhat more flexible in analysis of input strains. However, the ubiquitination state of the substrates at the start of the assay is available in our approach and cryptic in the radiochemical method. Furthermore, the higher amount of retrotranslocated material in our studies allows for direct detection of the retrotranslocated substrate in the soluble fraction, thus providing direct evidence of full dislocation of a polytopic ERAD substrate. In addition, the elevated levels of Hrd1p in our protocol provide a useful internal control, since Hrd1p undergoes Ubc7p-dependent self-ubiquitination in addition to transfer to substrates under study. Thus, both approaches have distinct advantages, and the successful analysis of ERAD mechanisms will benefit from the use of each.

In both mammals and yeast, the AAA-ATPase Cdc48p/p97 is a key component of the postubiquitination step in ERAD of multiple substrates. Cdc48p was similarly required for the complete removal of Hmg2p-GFP from the ER membrane. Despite there being an ER-bound pool of Cdc48p/p97 (37), the cytosolic Cdc48p was the most important source of this activity. Perhaps Cdc48p plays a role in stabilizing the retrotranslocated Hmg2p-GFP, so it must be replenished from the soluble pool as the reaction proceeds, as has been proposed from structural studies of the mammalian p97 protein's role in ERAD (56).

Cdc48p AAA-ATPase is thought to power retrotranslocation. By capitalizing on the cell biology of the retrotranslocation reaction and the differing requirements for ATP by E1 and Cdc48p, we directly demonstrated an ATP requirement for

Hmg2p-GFP retrotranslocation. This separation depended on using AMP-PNP during the retrotranslocation phase of an experiment to show the specific need for a β - γ bond in this step. Interestingly, the simple method of separating ubiquitination from retrotranslocation by use of AMP-PNP instead of ATP in the complete reaction was not feasible, because AMP-PNP only poorly supported Hmg2p-GFP ubiquitination in the reconstituted HRD reactions.

This unexpected, HRD-specific requirement for the β - γ bond of ATP may be due to a requirement for Cdc48p in initiating Hmg2p-GFP ubiquitination. Consistent with this idea, *in vitro* Hmg2p-GFP ubiquitination was lower in reactions with *cdc48-2* preparations. It has been posited that Cdc48p may play a role in major histocompatibility complex I recognition as well as retrotranslocation in the US2- and US11-dependent pathway (35), and other AAA-ATPases have been implicated in the recognition of misfolded proteins for destruction (57, 58). This additional role for Cdc48p will be investigated in the future. It is also possible that Cdc48p-dependent retrotranslocation allows the movement of luminal lysines to the cytoplasmic face during ubiquitination, thus increasing the extent of ubiquitination observed when Cdc48p is fully functional. The *in vitro* approach makes the separation of such intertwined functions feasible.

A number of studies have implicated the ER-localized Ubx2p as an ER receptor for soluble Cdc48p. We directly tested this idea and found that microsomal Ubx2p is required for retrotranslocation of both Hmg2p-GFP and Hrd1p itself. Although the effects of Ubx2p are quite clear *in vitro*, *in vivo* Hmg2p-GFP degradation was slowed more by the partial loss of function *cdc48-2* mutant than by a complete *ubx2Δ* null (Fig. 3A compared with Fig. 5A). This implies that other ways are available for Cdc48p to engage the ERAD machinery, consistent with the observation that loss of Ubx2p does not completely remove Cdc48p association with the ER membrane (44). Nevertheless, our results directly implicate Ubx2p as a Cdc48p receptor (43, 45). Perhaps our assay is more sensitive due to the dilution of the cytosol rendering the system more dependent on the ability of the Ubx2p microsomes to attract Cdc48p. Ubx2p functions are probably broader than Cdc48p anchoring, since we have observed that a *ubx2Δ* null has a profound up-regulation of the unfolded protein response that is much greater than that caused by strong ERAD-inhibiting mutants of Cdc48p.⁸ The *in vitro* assay is particularly useful when this is considered, since in intact cells, a *ubx2Δ* null mutant is causing ongoing strong regulatory responses that may cloud observation of its direct ERAD functions.

We examined the involvement of the ubiquitin-binding, proteasome delivery adaptors Rad23p and Dsk2p *in vitro*. Although current models predict that these soluble adaptors would have a role only after retrotranslocation, we observed that their absence caused a strong block to retrotranslocation. The Rad23p and Dsk2p adaptors are predicted soluble proteins, but we saw significant restoration of retrotranslocation when the microsomal fraction was the sole source of Rad23p and

⁸ R. M. Garza, B. K. Sato, and R. Y. Hampton, unpublished observation.

Dsk2p. Furthermore, cytosol devoid of Rad23p and Dsk2p supported a lesser extent of Hmg2p-GFP ubiquitination whether the microsomal fraction was wild-type or double null. This could be due to a role in recruiting the "E4" Ufd2p, which has been posited to enhance ubiquitination of ERAD substrates, including Hmg2p-GFP (39), or altered recruitment of the ERAD-implicated ubiquitin protease Ufd3p (59). Thus, it appeared that these adaptors have added roles in ERAD that impact both the extent of ubiquitination and retrotranslocation, in addition to their proposed role as proteasomal adaptors. One possibility is that these upstream effects are all caused by proteasome recruitment to the ER. The 26S proteasome has both associated E3 ligases and multiple AAA-ATPase activities that could affect the degree of substrate ubiquitination and assist in Cdc48p-dependent extraction of ERAD substrates, respectively. Whatever the mechanism, it is clear that these adaptors have more complex functions than previously appreciated from genetic analysis of intact cells.

One of the challenging open questions concerning ERAD is the mechanism of exit from the ER membrane, and a number of candidate channels have been proposed (60, 61). We directly examined both the pair of derlins, Der1p and Dfm1p, and Sec61p in our assay and confirmed that neither the double mutant *der1Δ dfm1Δ* nor the temperature-sensitive *sec61-2* mutant had any detectable effects on *in vitro* retrotranslocation of Hmg2p-GFP. This is consistent with our *in vivo* studies that similarly showed a lack of effect of the *der1Δ dfm1Δ* mutant or even the *der1Δ dfm1Δ sec61-2* triple mutant on *in vivo* degradation of Hmg2p-GFP (51).

One appealing idea is that the large transmembrane domain of Hrd1p functions as a channel. We tested this idea for Hrd1p by formation of the "self-destructive" Hmg1-Hrd1p protein with the ubiquitination activity of Hrd1p but lacking the Hrd1p transmembrane domain. Hmg1-Hrd1p underwent ERAD that required Cdc48p and the proteasome (Fig. 8). However, Hmg1-Hrd1p degradation was unaffected in both a *hrd1Δ* null and a *doa10Δ hrd1Δ* double null, indicating that delivery to the proteasome could occur without either of these ER ligase transmembrane regions being present in the cell. Consistently, full-length Hmg1-Hrd1p underwent Cdc48p-dependent *in vitro* retrotranslocation in an *hrd1Δ* null.

These studies indicate that none of the channel candidates show a role in Hmg2p-GFP retrotranslocation. Perhaps there is a yet undiscovered protein required for retrotranslocation that is essential to cells or a poor genetic target, making its isolation by screening difficult. It may further be that there are redundant routes of extraction, thus masking the effects of the loss of any one. Finally, it is possible that retrotranslocation of Hmg2p-GFP occurs in a way that does not require a channel but instead involves the recruitment of lipids to form a soluble intermediate. One version of this idea has been suggested in a recent essay (62). Although we find this possibility unlikely, it cannot be ruled out until the route or exit is understood by either discovery of the still cryptic channel or the complete reconstitution of the process in a pure system devoid of channel candidates.

Our studies directly demonstrated retrotranslocation of full-length Hmg2p-GFP. Recent work on the Ste6-166p transmembrane Doa10p substrate implied that this multispansing mem-

brane protein was similarly moved to the soluble fraction (55). Combined, these results indicate that movement of entire transmembrane substrates is commonly occurring in ERAD, as has been suggested from *in vivo* studies with CFTR-Δ508 in mammalian cells (63). It is not clear how the 8-spanning integral membrane protein Hmg2p-GFP remains soluble in the cytosol. It will be important to analyze the physical state and binding partners of this molecular species to gain insight into what processes and proteins are responsible for this heroic thermodynamic event.

This and other *in vitro* approaches will allow detailed mechanistic analysis of the ERAD pathway. Our future directions will include the analysis of the nature and composition of the retrotranslocated Hmg2p-GFP and the role of the sterol regulatory signals that control Hmg2p and Hmg2p-GFP degradation in coordinating this key step with the earlier events that are required for movement of substrates from the ER to their proteasomal destruction.

Acknowledgments—We thank Michael David (Division of Biological Sciences, University of California, San Diego) for use of the FACSCalibur flow cytometer, Alan Taylor (Tufts University) for K6W-ubiquitin, Rohan Baker (Australian National University) for the USP2-cc plasmid, and Ron Kopito (Stanford University) for a sample of the purified protease. R. Y. H. further acknowledges Robert W. Hampton (Impart Financial, Ft. Worth, TX) for advice on resource management and fiscal spirituality.

REFERENCES

- Hampton, R. Y. (2002) *Curr. Opin. Cell Biol.* **14**, 476–482
- Ahner, A., and Brodsky, J. L. (2004) *Trends Cell Biol.* **14**, 474–478
- Hampton, R. Y. (2002) *Annu. Rev. Cell Dev. Biol.* **18**, 345–378
- Song, B. L., Javitt, N. B., and DeBose-Boyd, R. A. (2005) *Cell Metab.* **1**, 179–189
- Amano, T., Yamasaki, S., Yagishita, N., Tsuchimochi, K., Shin, H., Kawahara, K., Aratani, S., Fujita, H., Zhang, L., Ikeda, R., Fujii, R., Miura, N., Komiya, S., Nishioka, K., Maruyama, I., Fukamizu, A., and Nakajima, T. (2003) *Genes Dev.* **17**, 2436–2449
- Swanson, R., Locher, M., and Hochstrasser, M. (2001) *Genes Dev.* **15**, 2660–2674
- Cheng, S. H., Gregory, R. J., Marshall, J., Paul, S., Souza, D. W., White, G. A., O'Riordan, C. R., and Smith, A. E. (1990) *Cell* **63**, 827–834
- Kopito, R. R. (1999) *Physiol. Rev.* **79**, Suppl. 1, S167–S173
- Berke, S. J., and Paulson, H. L. (2003) *Curr. Opin. Genet. Dev.* **13**, 253–261
- Thrower, J. S., Hoffman, L., Rechsteiner, M., and Pickart, C. M. (2000) *EMBO J.* **19**, 94–102
- Hershko, A., and Ciechanover, A. (1998) *Ann. Rev. Biochem.* **67**, 425–479
- Bays, N. W., Wilhovskiy, S. K., Goradia, A., Hodgkiss-Harlow, K., and Hampton, R. Y. (2001) *Mol. Biol. Cell* **12**, 4114–4128
- Medicherla, B., Kostova, Z., Schaefer, A., and Wolf, D. H. (2004) *EMBO Rep.* **5**, 692–697
- Jarosch, E., Taxis, C., Volkwein, C., Bordallo, J., Finley, D., Wolf, D. H., and Sommer, T. (2002) *Nat. Cell Biol.* **4**, 134–139
- Hiller, M. M., Finger, A., Schweiger, M., and Wolf, D. H. (1996) *Science* **273**, 1725–1728
- Ye, Y., Shibata, Y., Yun, C., Ron, D., and Rapoport, T. A. (2004) *Nature* **429**, 841–847
- Lilley, B. N., and Ploegh, H. L. (2004) *Nature* **429**, 834–840
- Plemper, R. K., Bohmler, S., Bordallo, J., Sommer, T., and Wolf, D. H. (1997) *Nature* **388**, 891–895
- Wiertz, E. J., Tortorella, D., Bogyo, M., Yu, J., Mothes, W., Jones, T. R., Rapoport, T. A., and Ploegh, H. L. (1996) *Nature* **384**, 432–438
- Kreft, S. G., Wang, L., and Hochstrasser, M. (2006) *J. Biol. Chem.* **281**,

Hrd1p-dependent Retrotranslocation of HMG-CoA Reductase

- 4646–4653
21. Flury, I., Garza, R., Shearer, A., Rosen, J., Cronin, S., and Hampton, R. Y. (2005) *EMBO J.* **24**, 3917–3926
22. Bazirgan, O. A., Garza, R. M., and Hampton, R. Y. (2006) *J. Biol. Chem.* **281**, 38989–39001
23. Hampton, R. Y., and Rine, J. (1994) *J. Cell Biol.* **125**, 299–312
24. Spang, A., and Schekman, R. (1998) *J. Cell Biol.* **143**, 589–599
25. Gardner, R., Cronin, S., Leader, B., Rine, J., and Hampton, R. (1998) *Mol. Biol. Cell* **9**, 2611–2626
26. Shearer, A. G., and Hampton, R. Y. (2004) *J. Biol. Chem.* **279**, 188–196
27. Cronin, S. R., Khoury, A., Ferry, D. K., and Hampton, R. Y. (2000) *J. Cell Biol.* **148**, 915–924
28. Bays, N. W., Gardner, R. G., Seelig, L. P., Joazeiro, C. A., and Hampton, R. Y. (2001) *Nat. Cell Biol.* **3**, 24–29
29. Gauss, R., Jarosch, E., Sommer, T., and Hirsch, C. (2006) *Nat. Cell Biol.* **8**, 849–854
30. Denic, V., Quan, E. M., and Weissman, J. S. (2006) *Cell* **126**, 349–359
31. Nishikawa, S. I., Fewell, S. W., Kato, Y., Brodsky, J. L., and Endo, T. (2001) *J. Cell Biol.* **153**, 1061–1070
32. Gardner, R. G., Swarbrick, G. M., Bays, N. W., Cronin, S. R., Wilhovsky, S., Seelig, L., Kim, C., and Hampton, R. Y. (2000) *J. Cell Biol.* **151**, 69–82
33. Carvalho, P., Goder, V., and Rapoport, T. A. (2006) *Cell* **126**, 361–373
34. Ryu, K. Y., Baker, R. T., and Kopito, R. R. (2006) *Anal. Biochem.* **353**, 153–155
35. Ye, Y., Meyer, H. H., and Rapoport, T. A. (2003) *J. Cell Biol.* **162**, 71–84
36. Flierman, D., Ye, Y., Dai, M., Chau, V., and Rapoport, T. A. (2003) *J. Biol. Chem.* **278**, 34774–34782
37. Hitchcock, A. L., Krebber, H., Fietze, S., Lin, A., Latterich, M., and Silver, P. A. (2001) *Mol. Biol. Cell* **12**, 3226–3241
38. Gauss, R., Sommer, T., and Jarosch, E. (2006) *EMBO J.* **25**, 1827–1835
39. Richly, H., Rape, M., Braun, S., Rumpf, S., Hoegel, C., and Jentsch, S. (2005) *Cell* **120**, 73–84
40. Shang, F., Deng, G., Liu, Q., Guo, W., Haas, A. L., Crosas, B., Finley, D., and Taylor, A. (2005) *J. Biol. Chem.* **280**, 20365–20374
41. Walden, H., Podgorski, M. S., and Schulman, B. A. (2003) *Nature* **422**, 330–334
42. Johnston, N. L., and Cohen, R. E. (1991) *Biochemistry* **30**, 7514–7522
43. Schubert, C., and Buchberger, A. (2005) *Nat. Cell Biol.* **7**, 999–1006
44. Wilson, J. D., Liu, Y., Bentivoglio, C. M., and Barlowe, C. (2006) *Traffic* **7**, 1213–1223
45. Neuber, O., Jarosch, E., Volkwein, C., Walter, J., and Sommer, T. (2005) *Nat. Cell Biol.* **7**, 993–998
46. Wilkinson, C. R., Seeger, M., Hartmann-Petersen, R., Stone, M., Wallace, M., Semple, C., and Gordon, C. (2001) *Nat. Cell Biol.* **3**, 939–943
47. Rao, H., and Sastry, A. (2002) *J. Biol. Chem.* **277**, 11691–11695
48. Kang, Y., Vossler, R. A., Diaz-Martinez, L. A., Winter, N. S., Clarke, D. J., and Walters, K. J. (2006) *J. Mol. Biol.* **356**, 1027–1035
49. Lilley, B. N., and Ploegh, H. L. (2005) *Proc. Natl. Acad. Sci. U. S. A.* **102**, 14296–14301
50. Ye, Y., Shibata, Y., Kikkert, M., van Voorden, S., Wiertz, E., and Rapoport, T. A. (2005) *Proc. Natl. Acad. Sci. U. S. A.* **102**, 14132–14138
51. Sato, B. K., and Hampton, R. Y. (2006) *Yeast* **23**, 1053–1064
52. Gardner, R. G., Shearer, A. G., and Hampton, R. Y. (2001) *Mol. Cell Biol.* **21**, 4276–4291
53. Gardner, R. G., and Hampton, R. Y. (1999) *EMBO J.* **18**, 5994–6004
54. Plemper, R. K., Bordallo, J., Deak, P. M., Taxis, C., Hitt, R., and Wolf, D. H. (1999) *J. Cell Sci.* **112**, 4123–4134
55. Nakatsukasa, K., Huyer, G., Michaelis, S., and Brodsky, J. L. (2008) *Cell* **132**, 101–112
56. DeLaBarre, B., Christianson, J. C., Kopito, R. R., and Brunger, A. T. (2006) *Mol. Cell* **22**, 451–462
57. Ye, Y. (2006) *J. Struct. Biol.* **156**, 29–40
58. Ito, K., and Akiyama, Y. (2005) *Annu. Rev. Microbiol.* **59**, 211–231
59. Rumpf, S., and Jentsch, S. (2006) *Mol. Cell* **21**, 261–269
60. Plemper, R. K., and Wolf, D. H. (1999) *Mol. Biol. Rep.* **26**, 125–130
61. Scott, D. C., and Schekman, R. (2008) *J. Cell Biol.* **181**, 1095–1105
62. Ploegh, H. L. (2007) *Nature* **448**, 435–438
63. Johnston, J. A., Ward, C. L., and Kopito, R. R. (1998) *J. Cell Biol.* **143**, 1883–1898

SUPPLEMENTAL DATA

Table S1. Yeast strains used. Background genotype for cytosol and microsome strains in bold. Mutant strains used in the in vitro retrotranslocation assay were derived from this *ubc7Δ*, *hrd1Δ*, and *pep4Δ* background.

Name	Genotype
RHY 4288	<i>α ade2-101 met2 lys2-801 his3Δ200 trp1::hisG leu2Δ pep4Δ::HIS3 hmg2Δ::1myc-HMG2 hrd1Δ::kanMX ubc7Δ::LEU2</i>
RHY 4295	<i>trp1::hisG::TDH3_{PROM}-UBC7-2HA</i>
RHY 2923	<i>ura3-52::URA3::TDH3_{PROM}-HMG2-GFP</i> <i>trp1::hisG::TDH3_{PROM}-HRD1-3HA</i>
RHY 5549	<i>hrd3Δ::NatR ura3-52::URA3::TDH3_{PROM}-HMG2-GFP</i> <i>trp1::hisG::TRP1::TDH3_{PROM}-HRD1-3HA</i>
RHY 5550	<i>cdc48-2::NatR ura3-52::URA3::TDH3_{PROM}-HMG2-GFP</i> <i>trp1::hisG::TRP1::TDH3_{PROM}-HRD1-3HA</i>
RHY 5551	<i>cdc48-2::NatR ura3-52::URA3::TDH3_{PROM}-HMG2-GFP</i> <i>trp1::hisG::TRP1::TDH3_{PROM}-UBC7-2HA</i>
RHY 5040	<i>cdc48-3::NatR ura3-52::URA3::TDH3_{PROM}-HMG2-GFP</i> <i>trp1::hisG::TRP1::TDH3_{PROM}-HRD1-3HA</i>
RHY 4929	<i>cdc48-3::NatR ura3-52::URA3::TDH3_{PROM}-HMG2-GFP</i> <i>trp1::hisG::TRP1::TDH3_{PROM}-UBC7-2HA</i>
RHY 6660	<i>ubx2Δ::NatR ura3-52::URA3::TDH3_{PROM}-HMG2-GFP</i> <i>trp1::hisG::TRP1::TDH3_{PROM}-HRD1-3HA</i>
RHY 6397	<i>rad23Δ dsk2Δ::NatR ura3-52::URA3::TDH3_{PROM}-HMG2-GFP</i> <i>trp1::hisG::TRP1::TDH3_{PROM}-HRD1-3HA</i>
RHY 6394	<i>rad23Δ dsk2Δ::NatR ura3-52::URA3::TDH3_{PROM}-HMG2-GFP</i> <i>trp1::hisG::TRP1::TDH3_{PROM}-UBC7-2HA</i>
RHY 6065	<i>dfm1Δ der1Δ::NatR ura3-52::URA3::TDH3_{PROM}-HMG2-GFP</i> <i>trp1::hisG::TRP1::TDH3_{PROM}-HRD1-3HA</i>
RHY 6066	<i>sec61-2::NatR ura3-52::URA3::TDH3_{PROM}-HMG2-GFP</i> <i>trp1::hisG::TRP1::TDH3_{PROM}-HRD1-3HA</i>
RHY 7207	<i>ura3-52::URA3::TDH3_{PROM}-1myc-HMG1_{TM}-HRD1_{RING}-3HA</i>
RHY 7370	<i>cdc48-2::NatR</i> <i>ura3-52::URA3::TDH3_{PROM}-1myc-HMG1_{TM}-HRD1_{RING}-3HA</i>

RHY 3970 *a ade2-101 met2 lys2-801 his3Δ200 trp1::hisG leu2Δ
ura3-52::URA3::TDH3_{PROM}-HMG2-GFP*

RHY 5548 *a ade2-101 met2 lys2-801 his3Δ200 trp1::hisG leu2Δ
ura3-52::URA3::TDH3_{PROM}-HMG2-GFP cdc48-2::NatR*

RHY 3082 *α ade2-101 met2 lys2-801 his3Δ200
ura3-52::URA3::TDH3_{PROM}-HMG2-GFP*

RHY 5380 *α ade2-101 met2 lys2-801 his3Δ200
ura3-52::URA3::TDH3_{PROM}-HMG2-GFP ubx2Δ::NatR*

RHY 7521 *α ade2-101 met2 lys2-801 his3Δ200
ura3-52::URA3::TDH3_{PROM}-1myc-HMG1_{TM}-HRD1_{RING}-3HA*

RHY 7522 *α ade2-101 met2 lys2-801 his3Δ200 hrd1Δ::kanMX
ura3-52::URA3::TDH3_{PROM}-1myc-HMG1_{TM}-HRD1_{RING}-3HA*

RHY 7205 *α ade2-101 met2 lys2-801 his3Δ200 trp1::hisG leu2Δ
ura3-52::TDH3_{PROM}-HMG2cd::URA3::TDH3_{PROM}-1myc-HMG1_{TM}-HRD1_{RING}-
3HA hmg1Δ::LYS2 hmg2Δ::HIS3*

RHY 7439 *α ade2-101 met2 lys2-801 his3Δ200 trp1::hisG leu2Δ
ura3-52::TDH3_{PROM}-HMG2cd::URA3::TDH3_{PROM}-1myc-HMG1_{TM}-HRD1_{RING}-
3HA hmg1Δ::LYS2 hmg2Δ::HIS3 cdc48-2::NatR*

RHY 7257 *a ade2-101 met2 lys2-801 his3Δ200
ura3-52::TDH3_{PROM}-6myc-HMG2::URA3::TDH3_{PROM}-1myc-HMG1_{TM}-
HRD1_{RING}-3HA hmg1Δ::LYS2 hmg2Δ::HIS3*

RHY 7258 *a ade2-101 met2 lys2-801 his3Δ200
ura3-52::TDH3_{PROM}-6myc-HMG2::URA3::TDH3_{PROM}-1myc-HMG1_{TM}-
HRD1_{RING}-3HA hmg1Δ::LYS2 hmg2Δ::HIS3 hrd2-1*

Strain generation

Standard yeast techniques were used to integrate plasmids. The Hmg2p-GFP and Hmg1-Hrd1p plasmids were linearized with *StuI* and integrated at the *ura3-52* locus. *HRD1* constructs P_{TDH3} -*HRD1* and P_{TDH3} -*HRD1*-C399S (RING mutant) were linearized with *BsgI* and integrated at the *trp1* locus. Microsome and cytosol donor strains had deletions of *PEP4*, *HRD1*, and *UBC7* that were each plasmid-mediated. The remaining gene deletions were PCR product-mediated. Primers were designed to incorporate sequences specific to the 5' and 3' genomic regions of gene to be deleted into sequences that flank the nourseothricin resistance marker (*NatR*) in pRH1838. PCR was used to confirm deletions. Mutants *cdc48-2*, *cdc48-3* and *sec61-2* were introduced into strains using two PCR products. One PCR product is an amplification of the mutant allele synthesized with a primer that carries sequence that overlaps with the nourseothricin resistance marker PCR product. The second PCR product is an amplification of the nourseothricin resistance marker with a primer that carries sequence found downstream of the mutant allele. Instead of transforming with one PCR product amplified from the two individual products¹, both PCR products were simultaneously introduced to the cell by standard transformation techniques. Cells were selected for nourseothricin resistance, and then screened for temperature sensitive phenotype at the restrictive temperature 37°C, and confirmed by PCR. All primer sequences are available upon request.

In vitro Ubiquitination. Microsomes from a *ubc7Δ* null yeast strain expressing 3HA-Hrd1p from the *TDH3* promoter and Hmg2p-GFP from the *TDH3* promoter were prepared by glass bead lysis. For each 10 OD₆₀₀ units of log-phase cells, 200 μl of MF buffer (20 mM Tris pH 7.5, 100 mM NaCl, 300 mM sorbitol, with the following protease inhibitors (PIs): 1 mM phenylmethylsulphonyl fluoride, 260 μM 4-(2-aminoethyl) benzenesulfonyl fluoride hydrochloride, 100 μM leupeptin hemisulfate, 76 μM pepstatin A, 5 mM ε-aminocaproic

acid, 5 mM benzamidine, and 142 μ M N-tosyl-L-phenylalanine chloromethyl ketone) was added. At 4 °C, cells were lysed using hand vortexing for 6 x 1-minute intervals with 1-minute intervals on ice between each vortexing. The lysate was collected and pooled with two bead rinses with MF to give the crude microsomal lysate. The crude lysate was centrifuged for 5 seconds at room temperature at full speed (16,000 g). The resulting supernatant was transferred to a fresh tube. This was repeated until no cellular debris could be seen. Next, the microsomes were pelleted at 14,000 g for 45 minutes at 4 °C. The pellets were resuspended in B88 buffer (20 mM Hepes pH 6.8, 250 mM sorbitol, 150 mM KOAc, 5 mM MgOAc, 1 mM DTT, and PIs listed above), to a final concentration of 0.3 OD equivalent units/ μ L of B88.

Cytosol was prepared from strains overexpressing Ubc7p in a *hrd1 Δ ubc7 Δ* double null strain in a similar manner as the Schekman lab². Control cytosol was prepared in parallel from an otherwise identical *ubc7 Δ* null strain. 500 OD equivalents of cells were pelleted, rinsed twice with water, once with B88 buffer, and resuspended in 500 μ L of B88 buffer with PIs. The resuspended cells were transferred to a chilled mortar containing liquid nitrogen. The frozen cells were ground with a pestle until a fine powder resulted. The frozen powder was transferred to microfuge tubes and thawed on ice. Typically, 1 mM ATP from a 500 mM stock solution in H₂O pH 7.5 was added to thawed cytosol, however ATP was not added in AMP-PnP (Sigma Aldrich, St. Louis, MO) experiments. Once thawed, the crude cytosol lysate was centrifuged at 3,000 g for 5 min to remove large debris, and then the supernatant was transferred to a new tube and centrifuged at 20,000 g for 15 minutes. The resulting supernatant was then ultracentrifuged at 100,000 g for one hour. Protein concentration was measured using Bradford reagent. Cytosol concentrations were adjusted with B88 to 20-25 mg/mL for ubiquitination and retrotranslocation assays. MG-132 (Sigma Aldrich) was added to a final concentration of 300 μ M to microsomes and cytosol preparations.

One in vitro ubiquitination reaction typically consisted of 10 μ L microsomes and 12 μ L cytosol. ATP (500 mM stock) was added to each reaction to a final concentration of 30 mM. The

reactions were incubated for one hour at 30°C. The assay was stopped by solubilization with 200 µl of SUME (1% SDS, 8 M urea, 10 mM MOPS pH 6.8, 10 mM EDTA) with PIs and 5 mM N-ethylmaleimide (NEM). 600 µL immunoprecipitation buffer (IPB: 15 mM Na₂HPO₄, 150 mM NaCl, 2% Triton X-100, 0.1% SDS, 0.5% DOC, 10 mM EDTA, pH 7.5) with PIs and NEM was added and followed by addition of 15 µL-25 µL rabbit polyclonal antisera (anti-GFP, anti-loop, or anti-Hrd1p antisera; prepared in collaboration with Scantibodies, Inc., Santee, CA).

Precipitated material was collected by centrifugation and the supernatant was then transferred to a fresh tube. Immunoprecipitation (IP) incubation was carried out at 4°C for 12-16 hours with mixing. Protein A sepharose (GE Healthcare, Piscataway, NJ) was added to IPs. IPs were then incubated for 2-4 hours at 4°C with nutating. Protein A sepharose with bound protein was washed once with IPB and once with IPW (50 mM NaCl, 10 mM Tris, pH 7.5). Beads were aspirated to dryness and 55 µL 2X urea sample buffer (2XUSB: 8 M urea, 4% SDS, 10% β-mercaptoethanol, 125 mM Tris, pH 6.8) was added. The slurry was incubated at 50°C for 10 minutes. IPs were resolved by SDS-PAGE using 8% Tris-glycine gels, and then transferred to nitrocellulose. For anti-ubiquitin immunoblotting, nitrocellulose membranes were rinsed with water and autoclaved for 30 minutes at liquid setting and 15 minutes at gravity setting. Blocking and anti-ubiquitin (Zymed Laboratories, South San Francisco, CA) incubations were carried out with Tris-buffered saline containing 0.45% Tween-20 (TBS-HT) and 20% heat-inactivated bovine serum³. Blots were washed with TBS-HT. For anti-GFP or anti-HA blots, nitrocellulose membranes were blocked with 5% nonfat dried milk in Tris-buffered saline (TBS-T: 10 mM Tris, pH 8.0, 140 mM NaCl, 0.05% Tween 20) and anti-GFP (BD Biosciences, San Jose, CA) and anti-HA (Covance, Princeton, NJ) incubations were carried out in 2% non-fat dried milk in TBS-T. Goat anti-mouse conjugated with HRP (Jackson ImmunoResearch, West Grove, PA) recognized primary antibodies. Western Lightning chemiluminescence reagents (Perkin Elmer, Waltham, MA) were used for immunodetection.

1. Kitazono, A.A., Tobe, B.T., Kalton, H., Diamant, N. & Kron, S.J. Marker-fusion PCR for one-step mutagenesis of essential genes in yeast. *Yeast (Chichester, England)* **19**, 141-149 (2002).
2. Spang, A. & Schekman, R. Reconstitution of retrograde transport from the Golgi to the ER in vitro. *The Journal of cell biology* **143**, 589-599 (1998).
3. Swerdlow, P.S., Finley, D. & Varshavsky, A. Enhancement of immunoblot sensitivity by heating of hydrated filters. *Analytical biochemistry* **156**, 147-153 (1986).

Fig. S1. Time course of in vitro retrotranslocation. In vitro reactions were carried out with Hmg2p-GFP microsomes incubated with cytosol carrying Ubc7p for indicated number of minutes (Min), and then fractionated into supernatant (S) or pellet (P) fractions as described. Both ubiquitinated protein (top panel) and GFP immunoreactivity were immunoblotted to show the time course of both ubiquitination and the appearance of ubiquitinated Hmg2p-GFP in the S fraction.

Figure S1

